Effect of Low and Moderate Recycled Concrete Aggregate Replacement Levels on Concrete Properties

Contract #: 1036599 (An NRRA Research Project)

Task 4: Concrete Mixing and Testing

Principal Investigator
Rita Lederle
Assistant Professor
Department of Civil Engineering
University of St. Thomas
Phone: 651-962-7745
E-mail: rita.lederle@stthomas.edu

State's Technical Liaison
Bernard Izevbekhai
Minnesota Department of Transportation
Office of Materials and Road Research
Phone: 651-366-5454
E-mail: bernard.izevbekhai@state.mn.us

TABLE OF CONTENTS

TASK 4: Concrete Mixing and Testing 1
4.1. Materials 1
4.1.1. Aggregate 1
4.1.2. Mix Design 5
4.2. Methods 6
4.2.1. Mixing 6
4.2.2. Fresh Properties 6
4.2.3. Hardened Properties 7
4.3. Results 8
4.4. Acknowledgements 12
4.5. References 12

LIST OF TABLES

Table 1: Coarse Aggregate Properties 4
Table 2: Final Control Mix Design 5
Table 3: Testing Matrix 5
Table 4: Fresh Properties 9
Table 5: Compressive Strength 9
Table 6: Flexural Strength 10
Table 7: Surface Resistivity 10
Table 8: Hardened Properties 11
Table 9: DIC results 12

Table of Figures

Figure 1: Control coarse aggregate gradation 1
Figure 2: Control fine aggregate gradation (data provided by Cemstone) 2
Figure 3: Control aggregate tarantula curve 3
Figure 4: RCA and #67 control gradations 4

TASK 4: Concrete Mixing and Testing

In this task, concrete samples were cast and tested for fresh and hardened properties. A total of 13 mixes were tested: one control group and four different recycled concrete aggregates (RCAs), each with three replacement levels.

4.1. Materials

4.1.1. Aggregate

The control aggregate was a limestone coarse aggregate sourced from Cemstone, a local ready-mix supplier, from their Faulkstone location. Two different sizes of coarse aggregate from the same pit were blended to make the final coarse aggregate gradation, shown in Figure 1. This blend is composed of 76.4% aggregate meeting the #67 gradation, and 23.6% aggregate meeting the #4 gradation, with gradations defined by ASTM C33 [1].

The #4 as received had a significant amount of material retained on the 1in sieve, but very little retained on the 1¼ in sieve. To drastically reduce the amount of material needed for testing, all material retained on the 1¼ in sieve was removed from the control aggregate. This allowed 4 in diameter by 8 in high cylinders to be used instead of the larger 6 in diameter by 12 in high cylinders. The data shown in Figure 1 reflect the removal of this material.

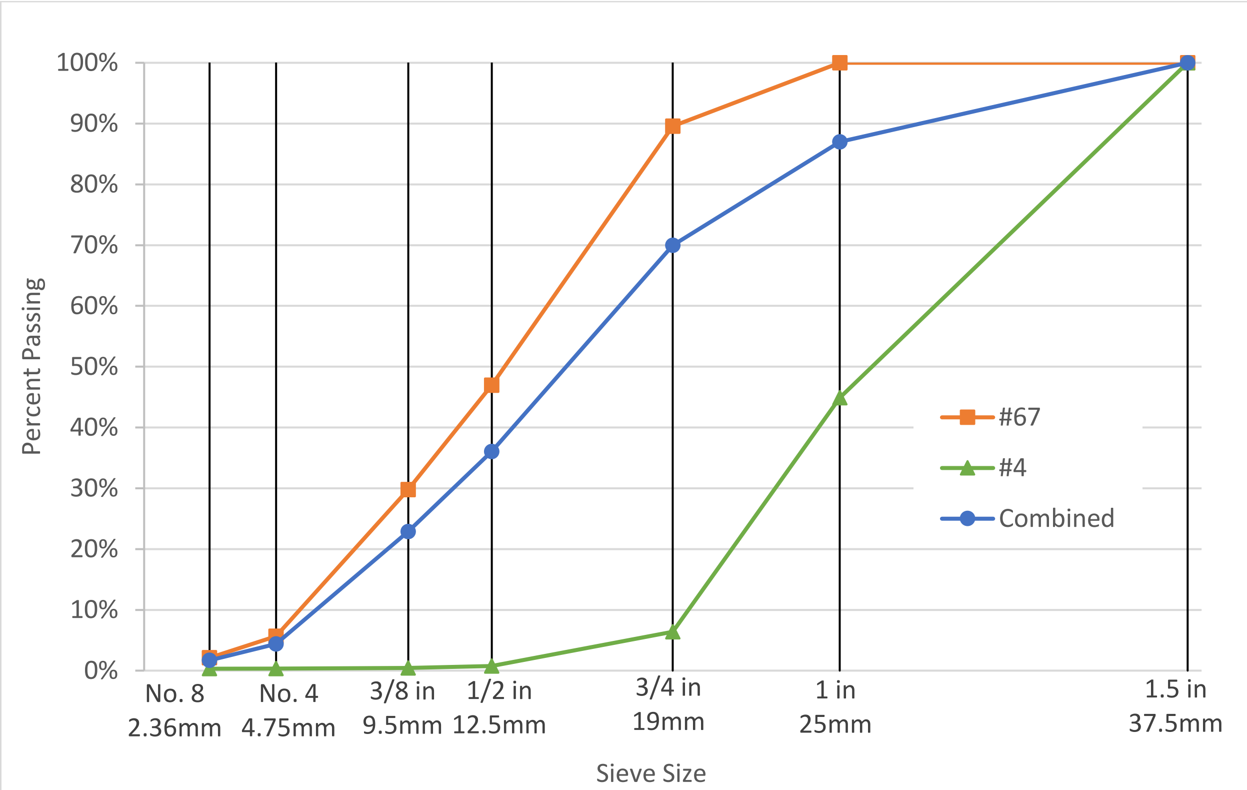

Figure 1: Control coarse aggregate gradation

Natural sand was selected as the fine aggregate sourced from the same supplier, from their Rosemont location. This sand was delivered in two separate batches, which were found to have slightly different gradations, as shown in Figure 2. The fineness moduli of sands A and B were

2.65 and 2.79 respectively, which is a 5.3% difference. Both sands met the ASTM C33 requirements for fine aggregate.

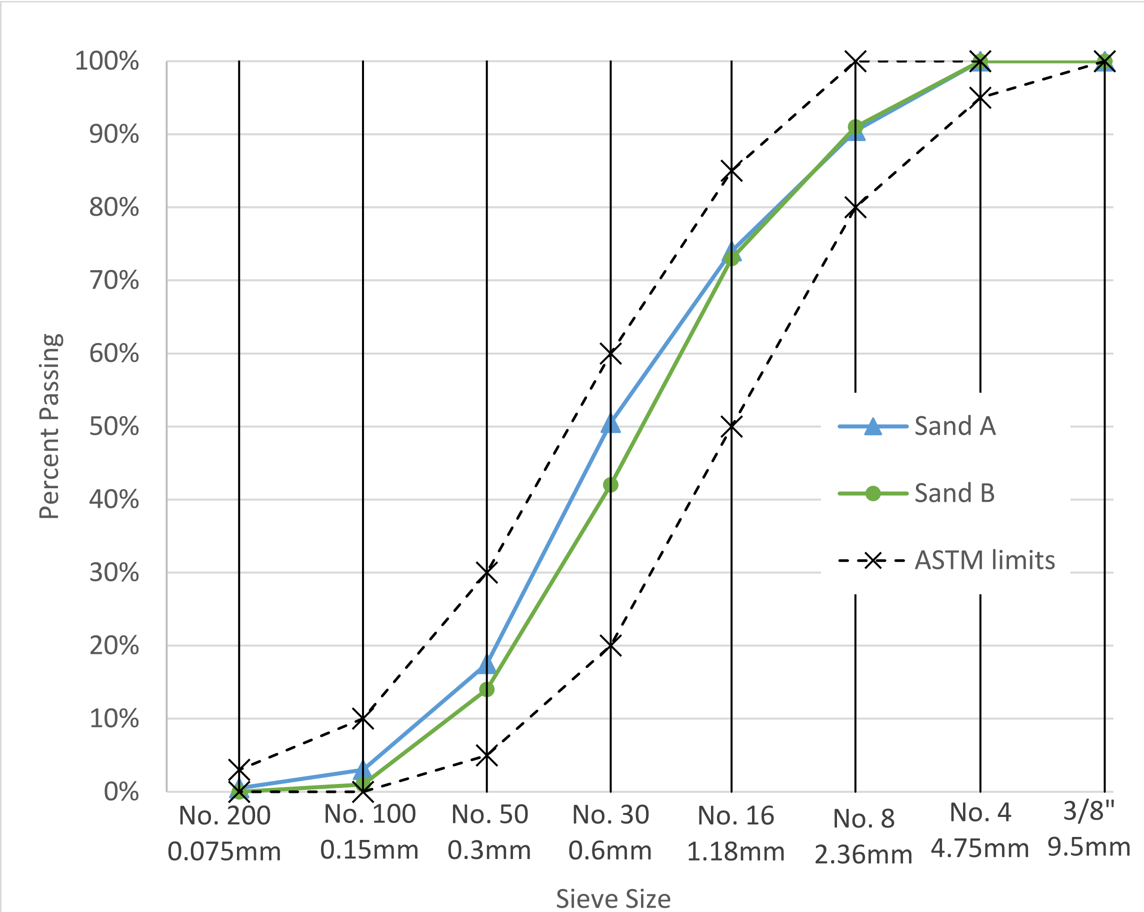

Figure 2: Control fine aggregate gradation (data provided by Cemstone)

The final aggregate blend was 45% sand and 55% blended coarse aggregate. This gradation meets the tarantula curve [2] for both sands A and B, as shown in Figure 3. This gradation also meets the tarantula curve requirements that coarse sand be greater than 15% and fine sand be between 24% and 34% for both sands A and B.

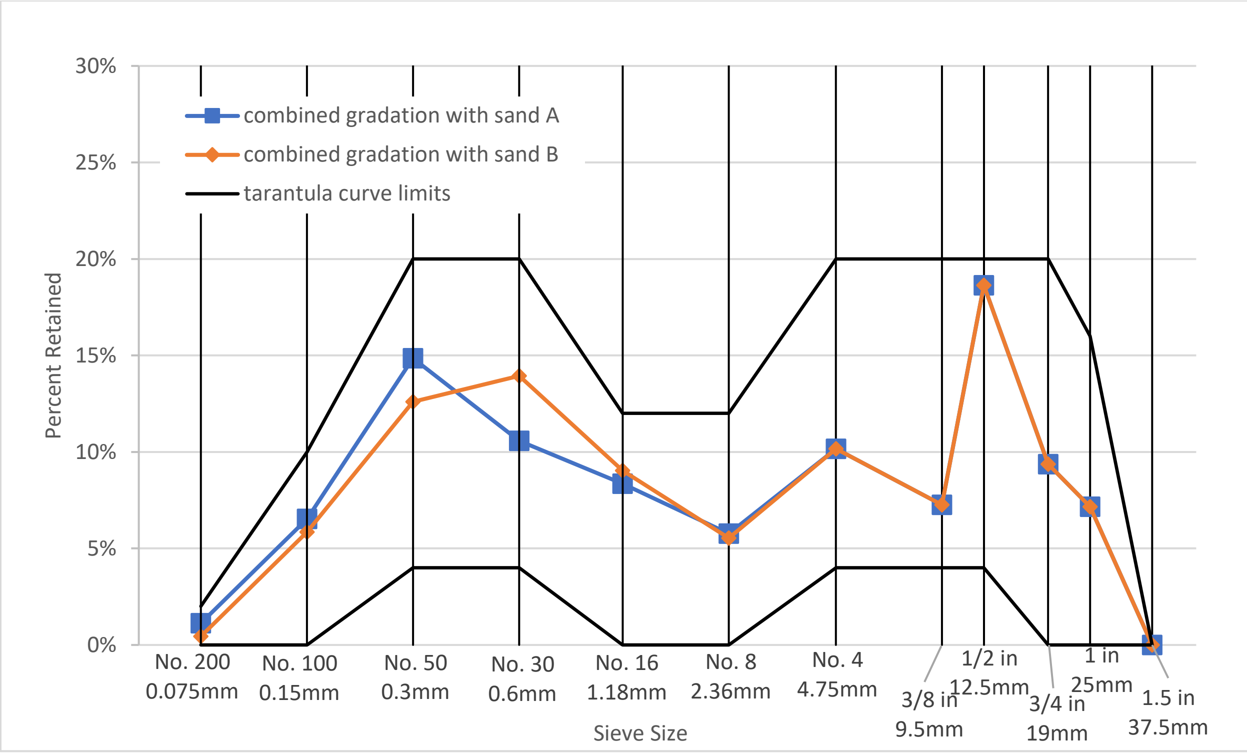

Figure 3: Control aggregate tarantula curve

Four RCA sources were selected with guidance from the technical advisory panel (TAP), as discussed in the Task 3 report. These materials were designated by their sources and can be described as follows:

1. Henderson: uncontrolled, mainly returned concrete and washout with some rubble from unknown sources
2. AVR: very controlled returned concrete
3. Aggregate Industries: multi-source from demolition waste, returned concrete, and washout
4. MoDOT: crushed airfield pavement made with limestone

The goal of RCA source selection was to ensure materials were representative of what producers would likely use if RCA were included in paving concrete. It was determined that sieving the RCAs to recreate the control aggregate gradation would be unrealistic because producers would not take this step during implementation. However, gradation does play a role in determining aggregate properties. In acknowledgement of this, only RCA materials meeting the #67 gradation were considered. While this may introduce some variation, it also gives results that are more realistic of field representation. None of the RCA supplied for this study was found to meet the #67 gradation criteria, but all were close. These aggregates are what producers supplied when asked for an RCA material meeting a #67 gradation and are likely representative of the aggregates that producers would be interested in using in concrete. Aggregate gradations were tested per ASTM C136 [3] and results are shown in Figure 4.

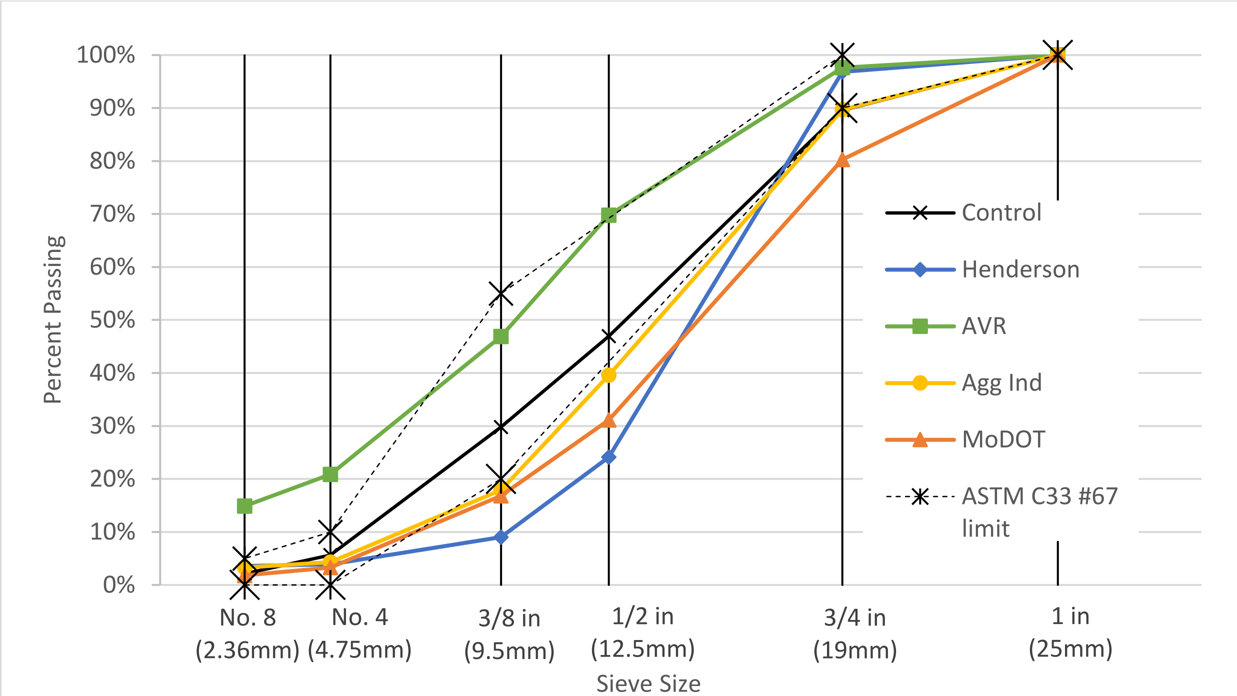

Figure 4: RCA and #67 control gradations

The coarse aggregate specific gravity and absorption capacity were tested in accordance with ASTM C127 [4]. The gradation testing including a wet wash per ASTM C117 [5] to determine the material passing the #200 sieve. The Missouri Department of Transportation conducted the micro-deval test in accordance with AASHTO T 327 [6] for all materials. Coarse aggregate properties are provided in Table 1.

Table 1: Coarse Aggregate Properties

Aggregate Source	Specific Gravity	Absorption Capacity	P-200	FM	Micro-deval
Control	2.68	1.06%	0.10%	3.78	10.4%
Henderson	2.32	5.32%	0.70%	3.77	21.4%
AVR	2.18	8.78%	2.89%	2.50	20.5%
Aggregate Industries	2.29	6.05%	0.67%	3.45	19.7%
MoDOT	2.40	3.50%	0.70%	3.67	14.4%

4.1.2. Mix Design

The mix design was developed in Task 3 and is repeated in Table 2 for convenience.

Table 2: Final Control Mix Design

Ingredient	lb/cy
Water	224
Cement	448
Fly ash	112
#67 coarse aggregate	1323
#4 coarse aggregate	410
Sand	1376
Admixture	oz/cwt
MRWRA	0.37
AEA	2.6

The testing matrix consisted of 13 total mixes: a control group and the four RCA materials, each at three different replacement levels. Based on the results of the literature review in Task 2, it was determined that RCA replacement levels of 20% or more can have an effect on concrete properties, depending on the RCA properties. Therefore, replacement levels of 5, 10, and 15% were considered. The final testing matrix is shown in Table 3.

Table 3: Testing Matrix

Aggregate source and type	Replacement level (by volume)	Designation
Control – virgin limestone	N/A	Control
Henderson – returned concrete with some unknown concrete rubble	5%	Henderson 5
	10%	Henderson 10
	15%	Henderson 15
AVR – unwashed, crushed returned concrete	5%	AVR 5
	10%	AVR 10
	15%	AVR 15
Aggregate Industries – multi-source, demolition waste, returned concrete, washout	5%	Agg Ind 5
	10%	Agg Ind 10
	15%	Agg Ind 15
MoDOT – crushed airfield pavement with limestone aggregate	5%	MoDOT 5
	10%	MoDOT 10
	15%	MoDOT 15

Aggregate replacement was done by volume, not weight, because RCA has a lower specific gravity than virgin aggregate due to the presence of the adhered paste. The #67 virgin material was replaced with RCA such that the total of virgin aggregate replaced was 5, 10, or 15%. This resulted in a constant weight and volume of the #4 control aggregate in the mix.

As discussed above, the sand was delivered in two batches, which had slightly different gradations. The Control, Henderson, AVR, AggInd5, and AggInd10 batches were made entirely with sand A. The AggInd15 batch was made with 96.3% sand A in the beams and 95.3% sand A for fresh testing and all other samples, with the remainder of the sand coming from sand source B. The difference in the percent of each sand used comes from different amounts of sand being required for moisture corrections. All the MoDOT batches were made entirely with sand B.

4.2. Methods

4.2.1. Mixing

Concrete was mixed in the St. Thomas Civil Engineering Lab in accordance with ASTM C192 [7]. For each RCA replacement level, the concrete was mixed in two separate batches to accommodate the mixer capacity. All of the concrete for the beams was mixed in one batch, and concrete for all other samples and fresh testing was mixed immediately afterwards. Generally there was sufficient concrete left from the beam batch to cast a few of the cylinders, with the remainder cast from the second batch. Due to mold availability, the control group beams were split into multiple batches instead of being cast from one single batch. Similarly, the shrinkage, freeze-thaw, and coefficient of thermal expansion samples for the control group and the shrinkage and freeze-thaw samples for the Henderson10 group were batched separately from the other samples.

Concrete samples for hardened testing were cast in accordance with their respective specifications and left covered in the lab for one day. Samples were demolded and placed in lime-water tanks to cure in accordance with ASTM C192 for the requisite number of days, depending on testing. All cylinders were 4in diameter x 8in high. Concrete beams had a 6in x 6in cross section. Freeze-thaw prisms were 4in x 3in x 16in and length change prisms were 4in x 4in x 11.25in with an effective gauge length of 10in. Sample sizes were selected based on the nominal maximum aggregate size of 1¼ in.

4.2.2. Fresh Properties

Fresh properties were tested immediately following mixing. Slump was tested in accordance with ASTM C143 [8]. Air content via the pressure method in accordance with ASTM C231 [9] with a Type B meter. Previous research has concluded that the pressure method can be used with RCA, though it does measure the total air content of the original and new pastes [10,11].

The SAM number was measured via the sequential pressure method in accordance with AASHTO TP118 [12], though the test often took longer than the specified 12 minutes to run. The same trained operator performed the SAM test on all mixes; this operator has a history of performing the test correctly.

The box test was run in accordance with AASHTO T396 [13]. Rather than evaluate the void rating immediately, photos were taken of each side of the concrete after the box sides were removed for later evaluation. Edge slump was evaluated on a binary of having occurred or not, rather than being measured. The threshold for edge slumping was 0.25in, as described in the test standard.

4.2.3. Hardened Properties

Compressive and flexural strength were tested in accordance with ASTM C39 [14] and C78 [15], respectively. Tests were conducted at 3, 7, 14, 21, 28, and 56 days after casting to investigate any effects on the rate of strength gain in addition to ultimate strength. The 21-day cylinders and 56-day beams for Henderson10 were inadvertently not tested. Results for compressive testing are reported as the average of four cylinders, except the 28 day strength, which is the average of five cylinders. The extra cylinder at 28 days was used for digital image correlation (DIC) testing. Results for the flexural test are the average of two beams.

The rate of compressive strength gain and flexural strength gain were also calculated. A trendline was fit to each data set and the derivative of this function was taken to determine the rate of strength gain. A logarithmic function was selected, providing an equation with the form $y = m*\ln(x) + b$. This resulted in a rate with the form m/x. The value of m was used to represent the rate of strength gain.

Surface resistivity was measured for all compressive test cylinders except those used for DIC because the paint needed for DIC testing blocked access to the surface. Resistivity testing was conducted in accordance with AASHTO T358 [16]. The recommended curing condition adjustment factor was applied to account for the fact that specimens were stored in a lime water bath instead of a moist cure room. Results are generally reported as the average of four cylinders. If any cylinder failed to meet the coefficient of variation criteria, that cylinder was excluded from the average. Based on the average resistivity value at a given concrete age, the qualitative risk of chloride ion penetration was estimated from the correlation provided in the test standard. The rate of increase in surface resistivity was also computed. A linear trendline was fit to each data set with the form $y = mx + b$. The derivative of this function, m, is the rate.

Elastic modulus and Poisson’s ratio were measured at 28 days in accordance with ASTM C469 [17]. Results are reported as the average of two tests.

Coefficient of thermal expansion (CTE) was measured in accordance with AASHTO T336 [18] and is reported as the average of two cylinders tested. Because only one cylinder could be tested at a time and the test took an entire day, not all tests were conducted at 28 days. Generally the first cylinder in a batch was tested at 28 days and the second at 29 or 30 days. However, if more than one batch was cast on the same day, some cylinders had to be tested even later. All cylinders were tested within a week of reaching 28 days. For the MoDOT 10 batch, only one cylinder was tested and no cylinders were tested for the Aggregate Industries 5 batch.

Digital image correlation (DIC) is a non-contact full field optical imaging technique that can be used to visualize strain fields on a three-dimensional surface, such as a concrete cylinder. DIC was conducted on one cylinder per mix as part of the compression testing at 28 days. A speckle pattern was applied to a surface of the concrete using spray paint. The cylinder was then tested in compression following the standard ASTM C39 procedure [14]. During testing, the specimen was photographed using high speed cameras at a rate of one image per 0.2 seconds. The DIC system tracked the displacements of the speckles recorded in the images to provide measurements of displacements. A surface was fit across this field of displacement from which strains are then approximated [19–22].

For each test, the image just before failure and an image taken 50 frames (10 seconds) before that image were selected and the tensile strain fields in the lateral direction were computed. The time step just before failure was selected as the image before the image with a visible crack. For two of the tests (Control and AVR 5), there were no visible cracks on portion of the cylinder facing the camera. Instead, the before failure was selected as the image before the image corresponding to when the compression machine stopped applying load. A histogram of each strain field was constructed over a constant bin range. By superimposing these histograms for a given test batch, it is possible to see how the distribution of tensile strains changed as the specimen approached failure. The mean and maximum strain values were also computed for each strain field.

Unrestrained shrinkage testing was conducted by measuring length change in accordance with ASTM C157 [23]. Testing followed the specified regime except that all samples were tested three days after the 28-day moist cure period instead of four. Shrinkage strain was computed by dividing the measured length change by the gauge length of 10 inches. All specimens except Henderson 10, and MoDOT15 experienced an approximately four-day period of storage between 50% and 70% relative humidity instead of a constant 50% due to a malfunction of the cure chamber. A similar malfunction caused all specimens except MoDOT 15 to experience another 12-hour period of storage between 50 and 50% relative humidity and all specimens to experience an approximately 48 hour period of storage between 50 and 60% relative humidity and two separate approximately 12 hour periods of storage between 30 and 50% relative humidity. These periods of altered humidity occurred at different ages for each batch because they were mixed on different days. The ultimate shrinkage was reported as the average of three samples per mix. Values are reported at 140 days, but testing will continue and later values will be provided in the final report.

Freeze-thaw durability was tested in accordance with ASTM C666 with Procedure A [24]. Testing commenced after 14 days of curing in the lime water tanks. Because only five batches could be tested simultaneously, some samples had to be stored while others were tested. Samples were stored in a saturated, frozen state. A power outage in the testing room caused some samples to experience up to four days of storage at room temperature still in a saturated state during testing. This outage did not affect the freezer storing the samples awaiting testing. All samples were tested until 300 cycles because the relative dynamic moduli remained above 60% of the initial dynamic modulus for each sample. The Aggregate Industries 5 sample was tested at 310 cycles instead of 300, but the relative dynamic moduli for all samples of the batch were fairly consistent with measurements from several previous cycles, so it is unlikely this had a large impact on the results. The durability factor was reported as the average of three samples per batch.

4.3. Results

Results of all fresh and hardened testing are provided below. A value of N/A indicates test results were not available for that property for that batch. Analysis and discussion of results will be provided in Task 5.

The results of the fresh concrete testing are shown in Table 4. The super air meter results include an analysis of if the SAM number is likely correct or not. For the box test, edge slumping was evaluated as a binary. A box test score of 2 or less is considered acceptable for slipform paving [2,25]

Table 4: Fresh Properties

Batch	Slump	Air	Super Air Meter		Box Test	
			SAM number	SAM likely correct?	Box test score	Edge slumping present?
Control	1.25	6.7%	0.13	no	2.75	yes
Henderson 5	1.75	5.2%	0.48	yes	1.75	yes
Henderson 10	3.75	9.5%	0.11	no	1.00	no
Henderson 15	3	7.9%	0.17	yes	2.25	yes
AVR 5	2.5	7.0%	0.07	no	1.50	yes
AVR 10	5.25	9.8%	error	no	1.00	yes
AVR 15	1	6.1%	0.04	no	2.25	yes
Agg Ind 5	2.75	7.0%	0.19	yes	2.50	yes
Agg Ind 10	3	9.0%	0.12	yes	1.50	no
Agg Ind 15	2.25	7.5%	0.21	N/A	2.00	yes
MoDOT 5	3.5	10.0%	0.14	No	1.25	yes
MoDOT 10	4.25	8.5%	0.28	N/A	1.50	no
MoDOT 15	3.5	9.0%	0.33	N/A	1.75	yes

The results of the compressive strength testing with time are shown in Table 5. The rate of strength gain is also provided.

Table 5: Compressive Strength

Batch	Compressive Strength (psi) at Day						Rate of strength gain m (psi/ln(day))
	3	7	14	21	28	56	
Control	3054	3887	4468	5086	5643	6323	1137
Henderson 5	3036	3916	4624	5223	5516	6500	1175
Henderson 10	1879	2549	3088	N/A	3816	4468	888
Henderson 15	2606	3149	3973	4325	4756	5549	1021
AVR 5	2358	3459	4250	4557	4802	5599	1083
AVR 10	1985	2658	3109	3697	3662	4456	831
AVR 15	2760	3529	4278	4933	5221	6165	1172
Agg Ind 5	2684	3441	4062	4446	4759	5665	995
Agg Ind 10	2251	2864	3621	3835	4217	4814	886
Agg Ind 15	2674	3393	4029	4382	4790	5472	956
MoDOT 5	2091	2879	3295	3679	3743	4671	830
MoDOT 10	2178	2962	3600	3971	4560	5125	1022
MoDOT 15	2444	3351	3828	4245	4460	5111	893

The results of the flexural strength testing with time are show in Table 6. The rate of strength gain is also provided.

Table 6: Flexural Strength

Batch	Flexural Strength (psi) at Day						Rate of strength gain, m (psi/ln(day))
	3	7	14	21	28	56	
Control	463	479	550	627	614	730	93
Henderson 5	410	467	518	537	572	684	87
Henderson 10	403	494	539	572	630	N/A	94
Henderson 15	401	468	589	651	685	721	120
AVR 5	458	591	630	689	704	748	98
AVR 10	448	519	600	597	679	791	112
AVR 15	455	501	555	620	675	708	93
Agg Ind 5	520	570	640	719	758	816	108
Agg Ind 10	460	558	609	666	704	770	106
Agg Ind 15	513	557	609	665	714	753	87
MoDOT 5	477	502	558	646	620	718	84
MoDOT 10	448	467	561	626	657	663	87
MoDOT 15	438	522	610	617	633	752	101

The results of the resistivity testing with time are show in Table 7. Both the numerical value and the associated qualitative risk of chloride ion penetration are provided. H indicates a high risk of chloride ion penetration, M indicates moderate risk, and L indicates low risk.

Table 7: Surface Resistivity

Batch	Surface Resistivity (kΩ-cm) and Associated Risk Level at Day						Rate of Resistivity Gain (kΩ-cm/day)
	3	7	14	21	28	56	
Control	8.4 (H)	9.3 (H)	11.9 (H)	13.8 (M)	15.9 (M)	22.9 (L)	0.277
Henderson 5	7.6 (H)	9.8 (H)	11.1 (H)	12.3 (M)	14.4 (M)	21.6 (L)	0.255
Henderson 10	6.8 (H)	8.4 (H)	9.9 (H)	0 (H)	13 (M)	19.5 (M)	0.234
Henderson 15	7.6 (H)	9.6 (H)	11.1 (H)	12.5 (M)	13.2 (M)	22.4 (L)	0.268
AVR 5	7.4 (H)	9.1 (H)	10.9 (H)	11.5 (H)	12.8 (M)	18.8 (M)	0.204
AVR 10	6.5 (H)	8.3 (H)	9.3 (H)	11.1 (H)	11.9 (H)	17 (M)	0.189
AVR 15	7.2 (H)	8.7 (H)	10.4 (H)	11.6 (H)	13.2 (M)	20.8 (M)	0.251
Agg Ind 5	7.5 (H)	9.1 (H)	10.5 (H)	12.2 (M)	13.3 (M)	21.1 (L)	0.249
Agg Ind 10	7.2 (H)	9 (H)	10.4 (H)	13.5 (M)	13.3 (M)	21.4 (L)	0.259
Agg Ind 15	7.4 (H)	9.2 (H)	11.9 (H)	12.2 (M)	14.3 (M)	21.1 (L)	0.246
MoDOT 5	7.4 (H)	8.8 (H)	10.2 (H)	12.3 (M)	13.7 (M)	21.1 (L)	0.255
MoDOT 10	7 (H)	9.3 (H)	10.5 (H)	11.5 (H)	12.3 (M)	19.2 (M)	0.214
MoDOT 15	7.5 (H)	10 (H)	11.1 (H)	12.6 (M)	15 (M)	19.6 (M)	0.217

Hardened properties measured at 28 days, including elastic modulus, Poisson's ratio, and coefficient of thermal expansion are shown in Table 8. The values of compressive strength, flexural strength, and surface resistivity at 28 days repeated here for completeness. Values not measured at 28 days include the freeze thaw durability factor and shrinkage. Durability factor testing commenced at an age of 14 days for all samples (by either testing them immediately or storing them in the freezer until testing) but the age at the completion of testing (when the durability factor is calculated) varies depending on the length of the freeze-thaw cycles. For shrinkage, the value at 140 days is included. This test is ongoing and final values will be provided in a later report.

Table 8: Hardened Properties

Batch	Compressive strength (psi)	Flexural strength (ksi)	Elastic modulus (ksi)	Poisson's ratio	CTE (mm/ mm/°C)	Surface Resistivity (kΩ-cm)	Freeze thaw durability factor	Shrinkage (με)
control	5643	614	5576	0.22	8.93	15.9 (M)	103	-380
Henderson 5	5516	572	5213	0.20	9.12	14.4 (M)	94	-330
Henderson 10	3816	630	4647	0.21	9.43	13 (M)	92	-307
Henderson 15	4756	685	4797	0.21	9.70	13.2 (M)	88	-443
AVR 5	4802	704	4561	0.18	9.49	12.8 (M)	106	-427
AVR 10	3662	679	4016	0.19	9.59	11.9 (H)	93	-477
AVR 15	5221	675	4409	0.20	9.49	13.2 (M)	86	-413
Agg Ind 5	4759	758	5089	0.21	N/A	13.3 (M)	89	-417
Agg Ind 10	4217	704	4764	0.22	9.30	13.3 (M)	95	-457
Agg Ind 15	4790	714	5436	0.21	9.70	14.3 (M)	90	-463
MoDOT 5	3743	620	4575	0.22	9.39	13.7 (M)	91	-327
MoDOT 10	4560	657	4730	0.19	8.87	12.3 (M)	88	-337
MoDOT 15	4460	633	4904	0.20	9.40	15 (M)	101	-380

The results of the DIC testing are shown in Table 9. These results include the maximum and average values of field strain for the image just before failure and 50 frames (10 seconds) before that image. Histograms will be provided in the Task 5 report.

Table 9: DIC results

Batch	Just before failure		50 frames before failure	
	Strain field maximum (με)	Strain field average (με)	Strain field maximum (με)	Strain field average (με)
control	5483	585	5604	538
Henderson 5	11782	574	2272	57
Henderson 10	5014	686	6369	115
Henderson 15	6279	1160	2641	610
AVR 5	7741	305	1955	261
AVR 10	6124	1108	2615	371
AVR 15	7646	1073	1807	416
Agg Ind 5	8788	686	3589	368
Agg Ind 10	9169	933	5259	384
Agg Ind 15	4104	507	3407	263
MoDOT 5	6337	395	1234	184
MoDOT 10	3280	307	3246	228
MoDOT 15	2699	504	1828	304

Analysis, including a statistical analysis of the results to determine significance, will be provided in the Task 5 report.

4.4. Acknowledgements

Brett Trautman and the Missouri Department of Transportation conducted micro-deval testing for this project. Student workers Evan Selin, Luke Gross, Evan Peters, Colin Nilsen, Amanda Birnbaum, and Ahadu Kenebre conducted the remainder of the testing. Lab manager Charles Allhands assisted with lab work and coordination. Dr. Sarah Baxter assisted with the digital image correlation data processing

4.5. References

[1] ASTM, ASTM C33/C33M Standard Specification for Concrete Aggregate, ASTM International, West Conshohocken PA, 2018.

[2] M.D. Cook, A. Ghaeezadah, M.T. Ley, Russell, B.W., Investigation of Optimize Graded COncrete for Oklahoma - Phase 1, Oklahoma Department of Transportation, Oklahoma City, OK, 2013.

[3] ASTM, C136/C136M Standard Test Method for Sieve Analysis of Fine and Coarse Aggregates, ASTM International, West Conshohocken PA, 2014.

[4] ASTM, C127 Standard Test Method for Relative Density (Specific Gravity) and Absorption of Coarse Aggregate, ASTM International, West Conshohocken PA, 2015.

[5] ASTM, ASTM C117-17 Standard Test Method for Materials Finer than 75-µm (No. 200) Sieve in Mineral Aggregates by Washing, ASTM International, West Conshohocken PA, 2017.

[6] AASHTO, AASHTO T 327-22 Standard Test Method for Resistance of Coarse Aggregate to Degradation by Abrasion in the Micro-Deval Apparatus, American Association of State Highway and Transportation Officials, Washington D.C., 2022.
[7] ASTM, C192/C192M Standard Practice for Making and Curing Concrete Test Specimens in the Laboratory, ASTM International, West Conshohocken PA, 2019.
[8] ASTM, C143 Standard Test Method for Slump of Hydraulic-Cement Concrete, ASTM International, Westh Conshohocken PA, 2020. https://doi.org/10.1520/C0143_C0143M-15A.
[9] ASTM, C231/C231M Standard Test Method for Air Content of Freshly Mixed Concrete by the Pressure Method, ASTM International, West Conshohocken PA, 2022.
[10] Z. Yang, K. Overall, H. Brown, Use of Recycled Concrete Aggregate in Concrete Pavement Mixes, Tennessee Department of Transportation, Nashville TN, 2022.
[11] K.P. Verian, N.M. Whiting, J. Olek, J. Jain, M.B. Snyder, Using Recycled Concrete as Aggregate in Concrete Pavements to Reduce Materials Cost, Indiana Department of Transportation, Indianapolis IN, 2013.
[12] AASHTO, AASHTO TP118 Standard Method of Test for Characterization of the Air-Void System of Freshly Mixed Concrete by the Sequential Pressure Method, American Association of State Highway and Transportation Officials, Washington D.C., 2018.
[13] AASHTO, T396 Standard Method of Test for Evaluating the Workability of Slip Form Concrete Paving with the Box Test, American Association of State Highway and Transportation Officials (AASHTO), Washington DC, 2022.
[14] ASTM, C39: Standard Test Method for Compressive Strength of Cylindrical Concrete Specimens, ASTM International, West Conshohocken PA, 2018.
[15] ASTM, C78/C78M Standard Test Method for Flexural Strength of Concrete (Using Simple Beam with Third-Point Loading), ASTM International, West Conshohocken PA, 2018.
[16] AASHTO, AASHTO T358 Standard Method of Test for Surface Resistivity Indication of Concrete’s Ability to Resist Chloride Ion Penetration, American Association of State Highway and Transportation Officials, Washington D.C., 2017.
[17] ASTM, C469/C469M Standard Test Method for Static Modulus of Elasticity and Poisson’s Ratio of Concrete in Compression, ASTM International, West Conshohocken PA, 2014.
[18] AASHTO, AASHTO T336 Standard Method of Test for Coefficient of Thermal Expansion of Hydraulic Cement Concrete, American Association of State Highway and Transportation Officials, Washington DC, 2009.
[19] M.A. Sutton, W.J. Wolters, W.H. Peters, W.F. Ranson, S.R. McNeill, Determination of Displacments using an Improved Digital Correlation Method, Image and Vision Computing. 1 (1983) 133–139.
[20] M.A. Sutton, S.R. McNeill, J.D. Helm, Y.J. Chao, Advances in Two-Dimensional and Three-Dimensional Computer Vision, in: Photomechanics, Springer, Berlin, 2000: pp. 323–372.
[21] M.A. Sutton, C. Mingqi, W.H. Peters, Y.J. Chao, S.R. McNeill, Application of an Optimized Digital Correlation Method to Planar Deformation Analysis, Image and Vision Computing. 4 (1986) 133–139.
[22] H.A. Bruck, S.R. McNeill, M.A. Sutton, W.H. Peters, Digital Image Correlation Using Newton-Raphson Method of Partial Differential Correction, Experimental Mechanics. 29 (1989) 261–267.

[23] ASTM, C157/C157M Standard Test Method for Length Change of Hardened Hydraulic-Cement Mortar and Concrete, ASTM International, West Conshohocken PA, 2017.
[24] ASTM, C666/C666M Standard Test Method for Resistance of Concrete to Rapid Freezing and Thawing, ASTM International, West Conshohocken PA, 2015.
[25] AASHTO, AASHTO R101-22 Standard Practice for Developing Performance Engineered Concrete Pavement Mixtures, American Association of State Highway and Transportation Officials, Washington DC, 2022.